Supply Shocks and Inflationary Pressures in Global Value Chains: The Role of Network Centrality*

Yojiro Ito Harumasa Shirakawa

Abstract

We examine supply shock propagation through global value chains. To capture network heterogeneity, we construct a 30,000-node international input-output table by disaggregating sectoral data using trade microdata. Integrating this with supply shock identification leveraging micro-level quantity fluctuations, we find that high network centrality typically dampens price pass-through by one-third while amplifying quantity adjustments. During the COVID-19 recovery, however, these mechanisms were severely neutralized as physical bottlenecks restricted substitution pathways. These findings suggest that the network core's inherent stabilizing functions in normal times can act as an informational veil, masking the latent risks of non-linear inflationary surges as supply constraints eventually bind.

Keywords: Global Value Chains, Supply Shocks, Network Centrality, Inflation
JEL Classification: E31, F14, F41, D57, L14

*First version: July 2025. This version: February 2026. Preliminary and incomplete. Comments are welcome. The authors would like to thank Diego Comin for his helpful suggestions during the initial stages of this research, and Mototsugu Shintani for his valuable comments. We also thank staff at the Bank of Japan for their insightful discussions and feedback. The views expressed in this paper are those of the authors and do not necessarily reflect the official views of the Bank of Japan. Ito: Institute for Monetary and Economic Studies, Bank of Japan (Email: youjirou.itou@boj.or.jp). Shirakawa: Institute for Monetary and Economic Studies, Bank of Japan (Email: harumasa.shirakawa@boj.or.jp).

1 Introduction

The global inflationary episode in the aftermath of the COVID-19 pandemic has fundamentally reshaped our understanding of macroeconomic stability, highlighting the profound impact of supply chain disruptions. As production processes have become increasingly fragmented across national borders, Global Value Chains (GVCs) have evolved from mere conduits of trade into complex filters of global shocks. While recent literature has extensively documented the role of GVCs in transmitting shocks, we still lack a micro-founded understanding of how the network's structural topology modulates price and quantity adjustments. Crucially, the mechanism through which specific network nodes can either amplify or dampen inflationary signals remains a "black box" in contemporary macroeconomics.

A primary obstacle to understanding these mechanisms has been the dual limitation of existing data resolution and identification universality. First, standard international input-output (ICIO) tables, such as the OECD ICIO, rely on aggregate sectors that mask critical heterogeneity. As Antras et al. (2012) highlight, such coarse classifications prevent researchers from identifying specific "micro-bottlenecks"—systemically pervasive intermediate goods (Jones, 2011; Barrot and Sauvagnat, 2016) like semiconductors that function as the infrastructure of global production. Second, even when high-resolution data are available, the causal identification of shocks has remained restricted to specific empirical domains. While a growing literature has adopted empirical designs based on high-dimensional fixed-effects (HDFE) or leave-one-out (LOO) strategies to isolate exogenous shocks, their application has remained largely domain-specific. Prominent examples include the analysis of firm-level price pass-through within a single economy (Amiti, Itskhoki, and Konings, 2019) or the industry-level propagation of final demand shocks (Ferrari, 2025). This absence of a universal, supply-side identification framework applicable across the entire spectrum of traded goods has prevented a systematic mapping of idiosyncratic production disruptions onto the global network.

We address these fundamental challenges by developing an empirical framework that integrates high-resolution trade microdata with a comprehensive identification engine. First, we construct a "high-granularity ICIO table" by systematically disaggregating standard ICIO structures along both the supply and use dimensions: we refine the supply side (rows) using bilateral trade flows at the Harmonized System (HS) 6-digit level and the use side (columns) by applying detailed industry production recipes. This procedure results in a massive global production matrix spanning 76 countries and 388 sectors with over 218 million linkages, enabling us to uncover "shadow hubs" that possess immense structural centrality despite modest trade values. Second, we generalize the logic of HDFE and LOO strategies into a universal, supply-side identification framework. Crucially, while existing frontier studies such as Ferrari (2025) identify shocks using industry-level trade values, we extend this methodology to the supply side by utilizing physical quantities across more than 5,000 product categories. By extracting idiosyncratic exporter-specific shifters from quantities rather than values, we provide

a consistent measure of supply shocks that is fundamentally decoupled from price fluctuations and destination-specific demand. This methodological advancement effectively transforms the theoretical concept of network propagation into a measurable empirical parameter, providing a general-purpose research design for analyzing shock transmission in global production networks.

Leveraging this framework, we document two distinct empirical regularities in shock propagation. First, we identify a persistent "structural buffer effect" in price formation: products with high structural centrality exhibit significantly dampened price increases in response to negative supply shocks. Quantitatively, for a product with centrality one standard deviation above the average, the price hike is mitigated by approximately one-third relative to the baseline. Notably, we find that this resilience was significantly attenuated during the COVID-19 recovery period, as the magnitude of global disruptions may nearly offset the inherent buffering capacity of the network core. Second, we find that GVC centrality typically amplifies quantity adjustments in the long run. This mechanism, however, was effectively paralyzed during the COVID-19 recovery period. We term this phenomenon "topological neutralization," as the network-driven amplification vanished, suggesting that the network's inherent capacity to provide alternative supply pathways was obstructed by pervasive physical bottlenecks.

These findings provide empirical validation for the theoretical tension between price rigidities and network-driven substitution. The structural buffering we observe aligns with the logic of Pasten, Schoenle, and Weber (2020), who demonstrate that central nodes characterized by price rigidities—or "sticky hubs"—can function as structural anchors for the aggregate price level. The pivotal role of these nodes may incentivize firms to maintain price stability through long-term relational contracts to safeguard future trade rents (Macchiavello, 2022), providing a micro-founded rationale for this structural stickiness. Conversely, the collapse of quantity amplification during the pandemic recovery provides empirical support for the non-linear propagation models of Baqaee and Farhi (2019, 2022). In their framework, the network's capacity to dissipate shocks hinges on the elasticity of substitution; when physical bottlenecks compromise this ease of substitution, the network ceases to act as a stabilizer. Our results suggest that "topological neutralization" is a manifest case of this theoretical nonlinearity, where supply-side constraints effectively choked off the substitution pathways typically afforded by central nodes.

These findings offer significant implications for the monitoring of global inflationary pressures. The persistent price-buffering role of structural anchors implies a potential "signal attenuation" where inflationary pressures remain latent in official indices even as physical disruptions accumulate. This structural decoupling suggests that price stability at the network's core can act as a veil, masking the accumulation of physical shortages—a scenario that mirrors the classic trade-off between price and quantity signals discussed by Weitzman (1974) and the literature on shadow prices (Bhattacharyya et al., 2019). By uncovering these latent dynamics, our framework provides a structural indicator to identify these hidden bottlenecks and assess the resilience of the global production network from a topological perspective.

Related Literature. Our work contributes to three strands of literature. First, we provide a large-scale empirical bridge to the theoretical literature on the network origins of macroeconomic fluctuations and granularity (Gabaix, 2011; Acemoglu et al., 2012; Carvalho, 2014; Baqaee and Farhi, 2019). While foundational studies establish how idiosyncratic shocks can aggregate into systemic volatility, their quantitative applications have been largely constrained by a reliance on standard, relatively coarse industry classifications. By scaling the network analysis to over 30,000 nodes, we offer a high-resolution empirical validation that uncovers "shadow hubs" and non-linearities that remain invisible at higher levels of aggregation.

Second, we add to the empirical literature identifying supply-side shocks through trade microdata (e.g., Hummels et al., 2014; Amiti, Itskhoki, and Konings, 2019; Ferrari, 2025). Unlike existing studies that are frequently restricted to single-country settings or specific event-studies, our framework implements a universal identification strategy across a global HS 6-digit panel. By extracting idiosyncratic exporter-specific shifters from physical quantities rather than values, we ensure our identified shocks are fundamentally decoupled from price fluctuations and destination-specific demand, providing a general-purpose research design applicable to the entire spectrum of traded goods.

Third, we contribute to the growing body of research on GVC dynamics during the COVID-19 pandemic and its inflationary consequences (e.g., Carvalho et al., 2021; di Giovanni et al., 2022; Santacreu and LaBelle, 2022). While these studies have successfully quantified the transmission of aggregate shocks, the specific mechanism through which network topology filters or masks price signals remains relatively under-explored. We extend this line of inquiry by uncovering "topological neutralization"—the collapse of substitution pathways under systemic pressure—and documenting the resulting "signal attenuation." By providing a structural explanation for why inflationary pressures may remain latent despite severe physical disruptions, we offer a micro-founded bridge between the network theories of price-setting (Pasten, Schoenle, and Weber, 2020) and the practical challenges of post-pandemic inflation monitoring.

The remainder of the paper is organized as follows. Section 2 describes the empirical framework and the identification strategy. Section 3 presents the structural properties of the GVC, followed by the empirical results on price responses and quantity adjustments. Section 4 concludes.

2 Empirical Framework

To investigate the propagation of supply shocks through global value chains (GVCs), we develop a multi-step empirical framework. We first describe the data sources and the construction of our high-granularity international input-output (ICIO) table. We then detail our identification strategy for isolating idiosyncratic supply shocks and our empirical specification for estimating trade elasticities.

2.1 Data Sources

Our analysis integrates three primary datasets, each serving a distinct role in our empirical framework.

First, we utilize the OECD Inter-Country Input-Output (ICIO) tables (2023 edition) as our global accounting backbone.[1] The dataset covers 76 economies and 45 aggregate sectors from 1995 to 2020. Second, we employ the CEPII BACI database, which provides bilateral trade flows at the Harmonized System (HS) 6-digit level (covering approximately 5,000 product categories) for the period 1995–2023. Third, we use the U.S. Bureau of Economic Analysis (BEA) Detailed Input-Output tables (2007, 2012, and 2017 benchmark years), which identify approximately 400 industries, as our reference technology.

Crucially, these datasets are utilized at different stages of our analysis. The high-granularity ICIO table, which serves as the basis for calculating network metrics such as centrality, is constructed by merging all three datasets (OECD ICIO, BACI, and BEA). In contrast, the idiosyncratic supply shifters described in Section 2.4 are estimated exclusively using the raw bilateral trade microdata from the BACI database. This distinction ensures that our identified supply shocks are derived directly from observed trade fluctuations, independent of any assumptions made during the ICIO disaggregation process.

2.2 A High-Granularity ICIO

To overcome the aggregation bias inherent in standard ICIO tables, we construct a "high-granularity ICIO" through a hybrid approach. This process disaggregates the broad sector-to-sector flows into product-to-industry transactions.

Formally, let i and j denote the exporter and importer countries, respectively. Let R and S denote the aggregate sectors in the ICIO, and let r and s denote the granular sub-sectors (products or industries) such that $r \in R$ and $s \in S$. We estimate the flow x_{ij}^{rs} from sub-sector r in country i to sub-sector s in country j as follows:

$$x_{ij}^{rs} = \left(\sum_{S} Z_{ij}^{RS} \right) \times \alpha_{ij}^{r} \times \beta_{r \to s} \tag{1}$$

where $\sum_S Z_{ij}^{RS}$ represents the total value of intermediate exports from sector R in country i to all industries in country j, extracted from the OECD ICIO. The term $\beta_{r \to s}$ is the technical allocation coefficient representing the share of product r used as an intermediate input by industry s, derived from the BEA Detailed Input-Output tables.

[1] We choose the OECD ICIO tables over the World Input-Output Table (WIOT) from the World Input-Output Database (WIOD), provided by the Groningen Growth and Development Centre at the University of Groningen, primarily due to their extended temporal coverage. While the latest WIOT (2016 release) only provides data up to 2014, the OECD ICIO covers the period up to 2020. This allows us to align our analysis with the full sample period of the trade data and to capture the structural shifts induced by the COVID-19 pandemic.

The allocation share α_{ij}^{r} captures the composition of sub-sector r within the aggregate sector R. For tradable sectors, α_{ij}^{r} is calculated as the bilateral trade share from the CEPII BACI database.[2] For non-tradable sectors and domestic transactions (where $i = j$), where product-level trade data are unavailable, we utilize the internal industry shares from the BEA tables to disaggregate the ICIO flows. While this assumes that the domestic industry composition mirrors that of the U.S., we expect this approximation to have a negligible impact on our findings, as GVC centrality and international inflation propagation are predominantly driven by cross-border trade in intermediate goods.

Following the "reference technology" assumption widely adopted in the trade literature (e.g., Nunn, 2007; Antràs and Chor, 2018), we assume that the detailed input requirements observed in the U.S. serve as a valid proxy for the technical coefficients of corresponding industries in other economies.

To align these coefficients with the temporal scope of our trade data (1995–2023), we utilize the BEA benchmark years (2007, 2012, and 2017) and apply linear interpolation for intermediate years, supplemented by constant back-filling for the pre-2007 period and forward-filling for the post-2017 period. Similarly, for the OECD ICIO tables, we assume that the structural linkages remain constant beyond 2020 and forward-fill the 2020 structure to cover the remaining years of our sample (2021–2023).

This construction procedure results in a massive global production network that significantly expands the resolution of existing ICIO tables. Specifically, our high-granularity ICIO covers 76 countries and 388 sectors, yielding approximately 30,000 unique country-sector nodes. By disaggregating the data to this level, we identify over 218 million potential international and domestic linkages. This high-resolution structure enables us to uncover the aforementioned "shadow hubs" and capture non-linear propagation effects that remain invisible at higher levels of aggregation.

2.3 Measuring GVC Centrality

To quantify the structural importance of each node within the global production network, we compute a measure of network centrality for each country-industry pair. The starting point for our centrality measure is the economic intuition that the structural importance of a supplier is endogenously determined by the importance of its customers. In a production network, a sector is considered central if it provides essential inputs to other highly central sectors, thereby acting as a critical hub for downstream value creation.

This recursive logic—where a node's influence is the sum of the influences of the nodes it supplies—is a hallmark of multisector models with input-output linkages, most notably formalized by Acemoglu et al. (2012). We define the centrality vector v as satisfying the

[2] A potential concern is that bilateral trade flows include both intermediate and final goods. In future iterations of this paper, we plan to refine this decomposition by excluding product categories primarily classified as final consumption goods to further isolate pure intermediate linkages.

following structural relationship:

$$v' = f' + \alpha v' W \tag{2}$$

where f is a vector representing the initial external impulse originating from each node, and W is the $N \times N$ global direct requirement matrix. We define each element of this matrix as $w_{ij} = x_{ij}/y_j$, representing the value of intermediate inputs from country-sector i required to produce one unit of country-sector j's gross output y_j. The parameter $\alpha \in (0, 1)$ serves as a decay factor reflecting the weight of intermediate linkages. By solving for v, we obtain:

$$v' = f'(I - \alpha W)^{-1} \tag{3}$$

where $(I - \alpha W)^{-1}$ is the global Leontief inverse matrix.

Expanding this relationship into an infinite series provides the economic intuition:

$$v' = f' + \alpha f' W + \alpha^2 f' W^2 + \alpha^3 f' W^3 + \dots \tag{4}$$

The first term, f', represents the direct impact of a supply-side impulse. The subsequent terms, $\alpha^n f' W^n$, capture the n-th order cascades as the shock ripples through downstream sectors and across national borders. A high centrality score indicates that a shock to a specific node has a large cumulative impact on the global economy through the entire infinite chain of subsequent production stages.

To isolate the pure structural centrality, we assume a uniform demand distribution by setting $f = \frac{1}{N}\mathbf{1}$. This ensures our metric is mathematically equivalent to Katz Centrality (Katz, 1953) and Forward Linkages Miller and Blair (2022). This formulation allows our measure to be interpreted as the principal eigenvector of the production network under a non-homogeneous impulse, identifying the stationary distribution of structural influence.

Due to the high dimensionality of our ICIO matrix, directly computing the Leontief inverse $(I - \alpha W)^{-1}$ is computationally prohibitive. In practice, we approximate v by iteratively summing the power series in Eq. (4) until the centrality scores converge, ensuring that we capture the full depth of the global value chain. By identifying nodes with the highest values in v, we structurally locate what we term *Shadow Hubs*: sectors that function as critical systemic conduits despite their modest trade volumes. In our baseline specification, we set $\alpha = 0.5$, consistent with the average share of intermediate inputs observed in our dataset.

2.4 Identification: Supply Shifters

The central empirical challenge in estimating trade elasticities is the simultaneity of supply and demand shocks. To address this, we isolate idiosyncratic supply-side fluctuations at the exporter-product level using a high-dimensional fixed-effects approach. This strategy allows us to extract a universal shifter applicable to all trade flows, overcoming the limitations of

"intermittent" instruments such as tariff changes that are often restricted to specific products or time periods.

We construct our supply shifter, $\hat{\eta}_{i,k,t}^{(-j)}$, for each exporter i, product k, and year t, utilizing the rich variation in bilateral trade microdata from the CEPII BACI database. Our identification strategy builds on the "leave-one-out" (LOO) logic that has become a standard practice in the international trade and labor literature to isolate idiosyncratic shocks (e.g., Autor et al., 2013; Hummels et al., 2014). Specifically, we follow the spirit of Amiti et al. (2019) and Ferrari (2025) in using high-dimensional fixed effects to capture exporter-specific shifts that are exogenous to a given destination. While the fundamental logic of using rest-of-the-world fluctuations is well-established, we introduce a critical refinement by extracting these shifters from a panel of export *quantities* ($\ln q$) rather than values. This distinction is vital: by relying on physical volumes, we ensure that the identified shifter reflects genuine shifts in production capacity and idiosyncratic productivity shocks, avoiding the mechanical contamination from price fluctuations that often plagues value-based instruments.

Formally, for each target importer j, we identify the exporter-specific supply shock by estimating a fixed-effects model on the panel of all bilateral trade flows excluding those directed to country j. Let $\mathcal{J}$ be the set of all countries in our sample. For a given target $j \in \mathcal{J}$, we estimate the following specification:

$$\Delta \ln q_{i,n,k,t} = \eta_{i,k,t}^{(-j)} + FE_{n,t} + \epsilon_{i,n,k,t}, \quad \forall n \in \mathcal{J} \setminus \{j\} \tag{5}$$

where $q_{i,n,k,t}$ is the import quantity of product k from country i to destination n in year t. The key parameter of interest is the estimated fixed effect $\hat{\eta}_{i,k,t}^{(-j)}$, which captures the idiosyncratic supply-side variation specific to exporter i for product k, estimated using the sample of all destination countries except j.

This leave-one-out sampling is essential for the exclusion restriction: by omitting the direct trade flows to country j, we ensure that the instrument $\hat{\eta}_{i,k,t}^{(-j)}$ is not contaminated by the idiosyncratic demand shocks or preferences of the importer j currently under analysis. One potential concern is that $\hat{\eta}_{i,k,t}^{(-j)}$ may still be correlated with global demand cycles specific to product k. We address this through a two-layered defense. First, the importer-year fixed effects ($FE_{n,t}$) in the shifter estimation absorb destination-specific macroeconomic shocks, ensuring that η is not driven by the aggregate business cycles of other importers. Second, and more importantly, our main 2SLS specification includes high-dimensional Industry-Year fixed effects. This controls for broader global demand shifts at the sectoral level, allowing us to identify price and quantity movements driven by exporter-specific supply capacity that deviates from global industry trends.[3]

[3] In future iterations of this paper, we plan to further strengthen this identification by implementing a region-level leave-one-out approach following Amiti et al. (2019) and exploring alternative specifications that include product-year fixed effects in the shifter estimation stage to fully isolate exporter-specific idiosyncratic shocks from global product cycles.

2.5 Empirical Specification

To identify how a product's structural importance in the global production network modulates the propagation of supply shocks, we employ a two-stage least squares (IV-2SLS) framework. This approach allows us to estimate the causal impact of exporter-side supply shocks on both import prices and quantities, and specifically, how these effects vary with the centrality of the traded product.

In the first stage, we examine the pass-through of supply shocks to import prices by estimating the following equation:

$$\Delta \ln p_{ijkt} = \beta_1 \hat{\eta}_{ikt}^{(-j)} + \beta_2 (\hat{\eta}_{ikt}^{(-j)} \times C_{it-1}) + FE_{it} + FE_{jt} + FE_{st} + \epsilon_{ijkt} \tag{6}$$

where p_{ijkt} is the unit price of product k from exporter i to importer j at time t. The term $\hat{\eta}_{ikt}^{(-j)}$ represents our leave-out supply shifter, and C_{it-1} is the structural centrality of product k in country i. We include exporter-year (FE_{it}) and importer-year (FE_{jt}) fixed effects to control for time-varying macroeconomic conditions in each market, and industry-year (FE_{st}) fixed effects (where s corresponds to the BEA-USIO industry classification) to account for global industry-specific shocks. The coefficient β_2 captures the "buffer effect." If high-centrality goods serve as systemic infrastructure for the global economy, their prices may exhibit greater stickiness—potentially due to the high social cost of price volatility or long-term contractual rigidities—leading to a negative β_2.

In the second stage, we estimate the quantity response to these predicted price changes:

$$\Delta \ln q_{ijkt} = \sigma_1 \Delta \ln \hat{p}_{ijkt} + \sigma_2 (\Delta \ln \hat{p}_{ijkt} \times C_{it-1}) + FE_{it} + FE_{jt} + FE_{st} + \nu_{ijkt} \tag{7}$$

where q_{ijkt} is the imported quantity and $\Delta \ln \hat{p}_{ijkt}$ is the predicted price change from the first stage. The coefficient σ_1 corresponds to the standard Armington elasticity. Our focus is σ_2, the "network amplification effect," which tests whether the structural importance of a node triggers a chain of substitution across downstream industries, resulting in an amplified aggregate quantity adjustment.

Our empirical framework provides two distinct contributions to the literature. First, by utilizing structural centrality derived from our high-granularity hybrid ICIO table, we explore the structural heterogeneity of shock propagation—specifically the tension between the "buffer effect" and the "choke point" hypothesis. High granularity is essential for this purpose, as standard ICIO tables are too coarse to accurately identify the systemic hubs that define the topology of GVCs.

Second, our identification strategy utilizes a supply-side shifter that leverages the rich variation in bilateral trade microdata. Traditional methods for estimating Armington elasticities—including the GMM approach of Feenstra (1994), the frameworks reviewed by Burstein and Gopinath (2014), or tariff-based instruments—often rely on selective policy changes or shocks limited to specific products. In contrast, our approach provides a universal measurement of

supply shocks across all traded categories, ensuring comprehensive coverage of the production network.

To ensure that our estimated coefficients on centrality are not capturing other confounding structural characteristics, we provide an extended analysis in the Appendix. Specifically, we estimate specifications that simultaneously control for upstreamness at the country-industry level, the Herfindahl-Hirschman Index (HHI) of destination market concentration, and each country's global export share within a given product category. These variables serve as proxies for industry-specific characteristics such as commodity-like nature, destination-specific market power, and the idiosyncratic influence of market leaders, respectively. By including these controls, we can isolate whether the observed effects are uniquely attributable to the network's structural topology rather than mere transactional scale, industry positioning, or market concentration. Furthermore, we document that the systemic paralysis observed during the COVID-19 recovery period extends to these alternative market stabilizers, providing rigorous evidence of the pervasive nature of supply chain disruptions.

3 Results

3.1 Structural Properties and Shadow Hubs

Before presenting our main estimation results, we provide descriptive evidence on the structural properties of the global production network. Our primary measure of interest is the structural centrality, calculated as the eigenvector of the global Leontief inverse under unit final demand ($F = 1$). This measure isolates the "pervasiveness" of a product—the degree to which it serves as a critical, common input across the global economy—independent of the scale of final consumption.

The skewed distribution of centrality. The descriptive statistics of structural centrality reveal a highly skewed, power-law-like distribution. As summarized in the statistics for 2019, the median centrality score is 0.57, while the mean is 0.76. Crucially, the maximum value reaches 51.10 (for the iron and steel sector in China), which is nearly two orders of magnitude higher than the median. This "fat-tail" property suggests that the GVC is anchored by a small number of ultra-central nodes that function as the systemic infrastructure of global production.

Decoupling from trade volume. Table 1 presents the top 30 sector-country pairs ranked by structural centrality for the year 2019, immediately preceding the global pandemic. The ranking is dominated by upstream intermediate sectors such as iron and steel mills, nonferrous metal smelting, and electronic components. A striking feature of this ranking is the frequent decoupling between structural importance and trade volume. We refer to these systemically essential but transactionally modest nodes as "shadow hubs."

Table 1. Top 30 Sectors by Structural Centrality (2019)

Rank	Country	Sector Name (NAICS-based)	Centrality	Trade Rank
1	CHN	Iron and steel mills and ferroalloy manufacturing	51.10	31
2	CHN	Fabric mills	46.26	18
3	CHN	Nonferrous metal (ex. aluminum) smelting	23.70	334
4	CHN	Broadcast and wireless communications equipment	22.35	2
5	RUS	Iron and steel mills and ferroalloy manufacturing	21.50	110
6	CHN	Semiconductor and related device manufacturing	21.27	6
7	RUS	Nonferrous metal (ex. aluminum) smelting	19.62	125
8	JPN	Iron and steel mills and ferroalloy manufacturing	18.85	68
9	DEU	Iron and steel mills and ferroalloy manufacturing	17.42	85
10	CHN	Leather and allied product manufacturing	17.36	12
11	RUS	Oil and gas extraction	16.72	4
12	ITA	Iron and steel mills and ferroalloy manufacturing	16.59	167
13	CHN	Other basic organic chemical manufacturing	15.81	23
14	CHN	Motor and generator manufacturing	14.78	155
15	CHN	Other electronic component manufacturing	14.42	17
16	TUR	Iron and steel mills and ferroalloy manufacturing	13.82	238
17	AUS	Iron, gold, silver, and other metal ore mining	13.36	14
18	CHN	Plastics material and resin manufacturing	12.83	222
19	KOR	Iron and steel mills and ferroalloy manufacturing	12.75	102
20	SAU	Oil and gas extraction	12.68	3
21	CHN	Aluminum product mfg. from purchased aluminum	12.37	243
22	IND	Iron and steel mills and ferroalloy manufacturing	12.24	275
23	DEU	Nonferrous metal (ex. aluminum) smelting	12.21	221
24	CHN	Synthetic rubber and artificial fibers mfg.	12.13	236
25	KOR	Semiconductor and related device manufacturing	12.04	7
26	RUS	Alumina refining and primary aluminum production	11.72	483
27	JPN	Nonferrous metal (ex. aluminum) smelting	11.57	251
28	CHN	Printed circuit assembly manufacturing	11.51	101
29	UKR	Iron and steel mills and ferroalloy manufacturing	10.77	285
30	SGP	Semiconductor and related device manufacturing	10.54	30

Notes: This table reports the top 30 sectors ranked by structural centrality for the year 2019. Centrality is the structural centrality score calculated under unit final demand ($F = 1$) based on our high-granularity hybrid ICIO table. Trade Rank refers to the global rank of the exporter-sector pair in terms of total export value in 2019.

For instance, China's nonferrous metal smelting sector ranks 3rd in global structural centrality, yet it possesses a relatively modest global trade rank of 334th in terms of export value. An even more extreme case of this decoupling is observed in Russia's alumina refining and primary aluminum production, which ranks 26th in centrality despite a trade rank of 483rd. Conversely, high-volume consumer goods or large-scale commodities often exhibit relatively lower structural centrality compared to these bottleneck inputs. This discrepancy underscores that transaction scale is an insufficient proxy for a sector's role as a structural anchor in the global supply chain. The identification of these shadow hubs provides the empirical foundation for our subsequent analysis: given their role as pervasive common inputs, the economic costs of price volatility or

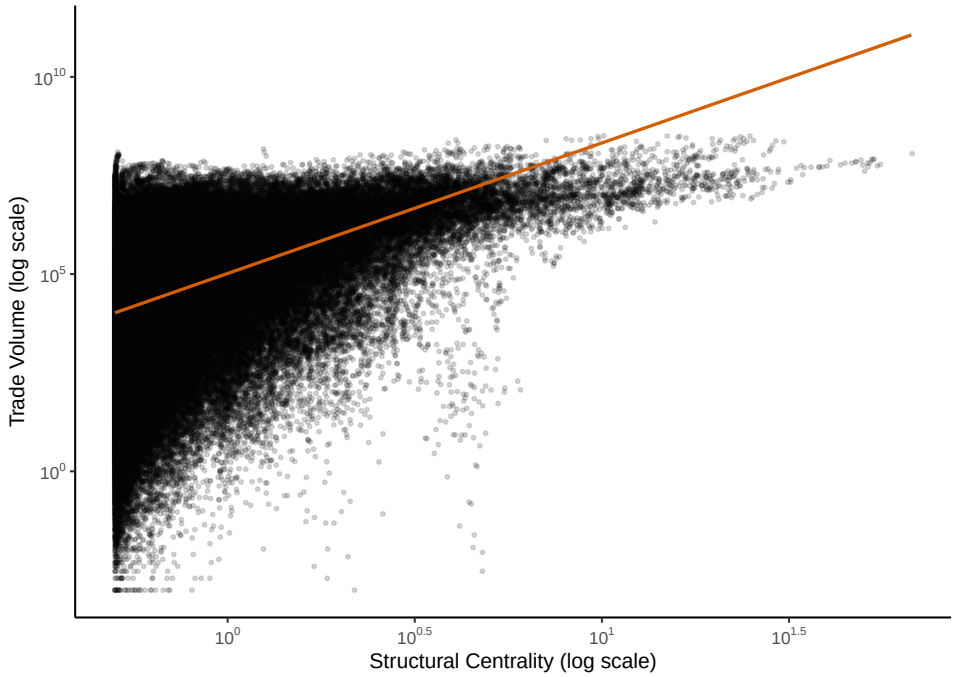


Figure 1. Structural Centrality vs. Trade Volume (1995–2023)
Notes: The figure plots structural centrality against trade volume for all sector-country pairs pooled over the period 1995–2023 ($N = 467,933$). The regression line indicates a positive correlation with a slope of 3.310 and $R^2 = 0.168$.

physical disruptions for these central goods are exceptionally high.

To formally examine this relationship, Figure 1 presents a log-log scatter plot of trade volume against structural centrality. While a baseline regression reveals a positive correlation, the significant vertical dispersion around the trend line confirms that structural centrality captures a distinct dimension of the GVC topology that is not subsumed by mere transaction scale. The observations located in the lower-right region of the plot represent these bottleneck sectors: products that are essential to a vast array of downstream processes despite their relatively modest trade values in the global market.

The identification of these shadow hubs provides the empirical foundation for our subsequent analysis. Given their role as pervasive common inputs, the systemic implications of price volatility for these central goods are potentially far-reaching. This structural positioning raises a fundamental empirical question: does network centrality serve to dampen or amplify the pass-through of supply shocks?

On one hand, the high social and economic costs of price instability for systemic inputs may provide an incentive for long-term contractual rigidities, positioning central nodes as structural anchors of price stability. On the other hand, the same centrality could transform these nodes into systemic choke points that accelerate the propagation of cost-push pressures across the network. This theoretical tension provides a structural rationale for how network centrality may modulate shock pass-through—a hypothesis formally evaluated in Section 3.2.

3.2 Centrality and the Structural Buffer Effect

The core of our empirical analysis follows a three-part logical structure: establishing the validity of identification, estimating primary trade parameters, and exploring structural shifts during the COVID-19 pandemic.

Price pass-through and the structural buffer effect. Table 2 reports the first-stage estimates of the pass-through of supply shocks to import prices. The baseline result in Column (1) shows that a negative supply shock leads to a statistically significant increase in import prices, confirming that our supply-side shifters effectively capture cost-push pressures. [4]

A key finding is the striking asymmetry revealed in Column (2). Specifically, while a negative supply shock carries a coefficient of -0.0097, the marginal effect of a positive shock is significantly offset by the interaction term ($+0.0066$), resulting in a much smaller net coefficient of -0.0031 for supply gluts. This implies that the upward price pressure from supply shortages is more than three times as strong as the downward pressure from gluts, a result consistent with the narrative of downward price rigidity in intermediate goods markets.

This stark asymmetry provides the empirical justification for the subsample analysis in Columns (3) and (4), where we separately examine how network topology modulates directional shocks. While the interaction with centrality is negligible for positive shocks (Column 3), it is positive and highly significant ($+0.0040$) for negative shocks (Column 4). The positive sign of this interaction is economically critical: since the supply shock η is negative, a positive coefficient on the interaction term effectively acts as a brake on the price increase. This suggests that for more central products, the cost-push pressure is endogenously dampened, confirming that the buffer effect is a mechanism specifically triggered during supply disruptions.

Quantitatively, for a product with structural centrality one standard deviation above the mean—representing a systemic hub that serves as a significantly more pervasive common input compared to the average product—the price hike triggered by a negative supply shock (-0.0114) is mitigated by approximately one-third relative to the baseline. This finding suggests that these central nodes effectively act as economic shock absorbers, where price stability is endogenously maintained to prevent cascading disruptions across the network. A potential explanation for this behavior is that because these goods are critical to a vast array of downstream industries, the social and economic costs of price volatility are exceptionally high. Such systemic importance may incentivize firms to adopt long-term contractual rigidities or other structural stabilizers, thereby dampening the pass-through of idiosyncratic shocks to ensure production continuity.

Armington elasticity and the network amplification effect. Table 3 presents the second-stage results for quantity responses. Our baseline IV-2SLS estimate for the Armington elasticity

[4] While the pass-through coefficient of -0.0071 is statistically robust, its modest magnitude reflects the idiosyncratic nature of the leave-one-out shifter, which isolates pure supply-side variation independent of aggregate demand trends.

Table 2. Price pass-through and the structural buffer effect

Dep. variable:	Change in import price ($\Delta \ln p$)			
	Baseline (1)	Asymmetry (2)	Positive (3)	Negative (4)
Supply shock (η)	-0.0071^{***}	-0.0097^{***}	-0.0045^{**}	-0.0114^{***}
	(0.0016)	(0.0017)	(0.0018)	(0.0017)
$\eta\times$ Pos. shock flag		0.0066^{***}		
		(0.0012)		
$\eta\times$ Centrality			0.0009	0.0040^{***}
			(0.0008)	(0.0008)
Fixed effects:				
Importer × Year	Yes	Yes	Yes	Yes
Exporter × Year	Yes	Yes	Yes	Yes
Industry × Year	Yes	Yes	Yes	Yes
Observations	125,560,334	125,560,334	49,740,382	75,819,952
R-squared	0.00925	0.00925	0.00935	0.00947

Notes: The table reports estimated coefficients from the first-stage price pass-through regressions for the full sample (1995–2023). Column (1) presents the baseline pass-through. Column (2) examines the asymmetry between positive and negative shocks. Columns (3) and (4) test the structural buffer effect by interacting the supply shock with topological centrality. Standard errors in parentheses are clustered at the exporter and industry levels. ***, **, and * denote significance at the 1, 5, and 10 percent levels.

is −4.758 (Column 1), which aligns with standard estimates found in the international trade literature (e.g., Feenstra, 1994; Burstein and Gopinath, 2014; Fontagné, Guimbard, and Orefice, 2022). The contrast with the OLS estimate of −0.6612 in Column (5) is stark. This significant discrepancy underscores that unobserved demand shocks frequently mask the true underlying price sensitivity of trade flows; specifically, the OLS coefficient suffers from attenuation bias because positive demand shocks drive simultaneous increases in both prices and quantities, creating a positive correlation that offsets the negative price elasticity and biases the coefficient toward zero.

Column (2) examines potential asymmetry in quantity responses. Unlike the price pass-through results, the interaction term for positive shocks is statistically insignificant (−0.1512), suggesting that the baseline demand elasticity remains relatively symmetric across directional shocks. However, a comparison of the subsample results in Columns (3) and (4) reveals a nuanced role for network topology. While the base elasticity for positive shocks is lower in absolute terms (−3.389) than for negative shocks (−4.756), the network amplification effect is more than twice as large in the negative subsample (−0.3292) compared to the positive one (−0.1275).

This finding indicates that structural centrality may play a decisive role in modulating quantity adjustments during supply disruptions. One potential interpretation of this result is that the network amplification of quantity adjustments occurs in tandem with, and perhaps contributes to, the structural buffer effect in prices. While the price hike for central goods is endogenously dampened, the quantity response appears disproportionately sensitive to even these mitigated price signals.

A possible mechanism underlying this observation is what we term a "chain of substitution" enabled by the production network. Given that central nodes are integrated into a vast array of downstream processes, a price increase—even if buffered—may function as a signal of systemic scarcity that triggers a synchronized search for alternatives across the entire downstream spectrum. As these substitution efforts propagate through the network tiers to preserve production continuity, the aggregate reduction in derived demand might, in turn, serve as a safety valve that further stabilizes prices by easing the immediate pressure on constrained supply.

3.3 Topological Neutralization during COVID-19

Table 4 investigates the structural stability of shock propagation by employing a triple interaction specification that compares the long-run baseline (1995–2019 and 2023) with the pandemic recovery period (2021–2022). To isolate the impact of supply-chain disruptions, we focus on the subsample of negative supply shocks ($\eta < 0$), excluding the transition year of 2020. The results reveal a profound regime shift: while the structural mechanisms governing the GVC were robust over the long run, they were significantly neutralized or eroded during the recovery period.

In the first stage (Column 1), we find that the structural buffer effect, a hallmark of the

Table 3. Demand elasticity and the network amplification effect

Dep. variable:	Change in import quantity ($\Delta \ln q$)				
	IV-2SLS				OLS
	Baseline (1)	Asymmetry (2)	Positive (3)	Negative (4)	Baseline (5)
Price change ($\Delta \ln \hat{p}$)	−4.758***	−5.223***	−3.389***	−4.756***	−0.6612***
	(0.7008)	(0.7490)	(0.9488)	(0.5425)	(0.0134)
$\Delta \ln \hat{p}\times$ Pos. shock		−0.1512			
		(0.3235)			
$\Delta \ln \hat{p}\times$ Centrality			−0.1275	−0.3292*	
			(0.0910)	(0.1761)	
Fixed effects:					
Importer × Year	Yes	Yes	Yes	Yes	Yes
Exporter × Year	Yes	Yes	Yes	Yes	Yes
Industry × Year	Yes	Yes	Yes	Yes	Yes
Observations	125,560,334	125,560,334	49,740,382	75,819,952	125,560,334
1st-stage F ($\Delta \ln \hat{p}$)	1,487.5	809.42	43.517	645.50	–
1st-stage F (Interact.)	–	17,966.6	1,366.5	5,473.5	–

Notes: Results for the second-stage demand elasticity regressions (1995–2023). Columns (1) to (4) instrument import prices with supply shocks (η) and their interactions. Column (5) provides OLS estimates for comparison. First-stage F-statistics indicate strong identification across all specifications. Standard errors in parentheses are clustered at the exporter and industry levels. ***, **, and * denote significance at the 1, 5, and 10 percent levels.

long-run baseline, was significantly attenuated during the recovery. The baseline interaction between supply shocks and centrality is positive and highly significant ($+0.0042^{***}$), confirming the inherent price-dampening role of central nodes. However, the triple interaction term for the recovery period is negative and significant (-0.0038^{*}), indicating that this price buffer was nearly entirely offset. This suggests that the capacity of central nodes to absorb cost-push pressures was severely compromised, likely due to the sheer magnitude of systemic disruptions that overwhelmed traditional price-stabilizing mechanisms.

The second-stage results (Column 2) exhibit an even more striking transformation. During the long-run baseline period, the interaction term between price changes and centrality is negative (-0.3576^{*}), consistent with the evidence that GVC centrality typically amplifies quantity adjustments through the pervasive "chain of substitution." However, during the recovery period, this amplification effect was not only neutralized but effectively reversed, as indicated by the large and positive triple interaction term ($+0.4690^{**}$).

We interpret this as a topological neutralization of the production network's adjustment margins. As indicated by the large and positive triple interaction term ($+0.4690^{**}$), the additional adjustment capacity typically afforded by high-centrality positions—the theoretical "chain of substitution"—was paralyzed during the recovery period. This suggests that while importers' fundamental sensitivity to price signals persisted, their ability to exploit topological advantages was obstructed by pervasive physical bottlenecks. In this environment, the network's structural heterogeneity disappeared, forcing all sectors to follow a uniform and constrained adjustment path regardless of their position in the GVC. These findings imply that the breakdown of this quantity-based "safety valve" likely contributed to the accumulation of latent inflationary pressures, as supply constraints could no longer be endogenously redistributed through the production network.

Table 4. Regime shift in GVC dynamics: Pre-COVID vs. COVID recovery

Dep. variable:	Stage 1: Price Change in price ($\Delta \ln p$) (1)	Stage 2: Quantity Change in quantity ($\Delta \ln q$) (2)
Supply shock (η)	-0.0117^{***}	
	(0.0017)	
$\eta\times$ Centrality	0.0042^{***}	
	(0.0009)	
$\eta\times$ Centrality $\times$ COVID	-0.0038^{*}	
	(0.0022)	
Price change ($\Delta \ln \hat{p}$)		-4.615^{***}
		(0.5030)
$\Delta \ln \hat{p}\times$ Centrality		-0.3576^{*}
		(0.1933)
$\Delta \ln \hat{p}\times$ Centrality $\times$ COVID		0.4690^{**}
		(0.2293)
Fixed effects:		
Importer $\times$ Year	Yes	Yes
Exporter $\times$ Year	Yes	Yes
Industry $\times$ Year	Yes	Yes
Observations	71,771,998	71,771,998
1st-stage F ($\Delta \ln p$)	–	430.87
1st-stage F (Shock $\times$ Cent)	–	4,549.7
1st-stage F (Triple Int.)	–	24,253.6

Notes: This table reports the results using a triple interaction specification to test for structural shifts during the COVID-19 recovery period (2021–2022). "COVID" is a dummy variable equal to one for the years 2021–2022. Column (1) presents the first-stage price pass-through, and Column (2) presents the second-stage quantity adjustments. All specifications are restricted to negative supply shocks ($\eta < 0$). Standard errors in parentheses are clustered at the exporter and industry levels. ***, **, and * denote significance at the 1, 5, and 10 percent levels.

4 Conclusion

This paper has investigated the propagation of supply shocks and their impact on inflationary pressures through Global Value Chains (GVCs). By utilizing highly granular trade microdata and a high-granularity hybrid ICIO table, we provide new evidence that the structural topology of the production network plays a decisive role in modulating both price pass-through and quantity adjustments.

Our findings document two primary empirical regularities that characterize the modern GVC. First, we identify a persistent "structural buffer effect," where products with high structural centrality—which we term "shadow hubs"—exhibit significantly dampened price increases in response to negative supply shocks. In the long-run baseline, this mechanism reduces price pass-through by approximately one-third. While these central nodes typically act as structural anchors for price stability, our evidence suggests this resilience was significantly attenuated during the COVID-19 recovery, as the sheer magnitude of global disruptions nearly offset the inherent buffering capacity of the network core.

Second, we find that GVC centrality typically amplifies quantity adjustments in the long run. This adjustment mechanism, however, was effectively paralyzed during the COVID-19 recovery period. This "topological neutralization" indicates that the network's inherent capacity to provide alternative supply pathways was obstructed by pervasive physical bottlenecks, forcing all sectors to follow a uniform and constrained adjustment path regardless of their position in the GVC.

These results offer significant implications for monetary policy and the monitoring of global supply-side inflation. By identifying systemic choke points that transaction-scale metrics often fail to capture, our framework provides a robust indicator for assessing the origins of inflationary pressures. For policymakers, these findings suggest a potential decoupling of price signals from physical shortages within the network's core. The persistent price-buffering role of shadow hubs implies that inflationary pressures may remain latent in official price indices while physical disruptions accumulate. This signal attenuation, combined with the temporary loss of the network's quantity-based "safety valve," creates a hidden vulnerability where localized shocks can transform into systemic supply-chain failures that are difficult for traditional demand-side policies to address.

The empirical regularities established in this paper provide a foundation for several promising avenues of future research. A natural next step is to develop a theoretical framework that formalizes the state-dependent nature of price buffering and the topological neutralization of quantity adjustments. Such a model would ideally incorporate micro-foundations of relational contracting and endogenous capacity constraints within a production network. Understanding the interaction between these structural frictions and network topology is essential for addressing the signal-extraction problem and designing optimal stabilization policies in an increasingly interconnected and supply-constrained global economy.

References

Acemoglu, D., Carvalho, V. M., Ozdaglar, A., & Tahbaz-Salehi, A. (2012). "The Network Origins of Aggregate Fluctuations." *Econometrica*, 80(5), 1977–2016.

Amiti, M., Itskhoki, O., & Konings, J. (2019). "International Shocks, Variable Markups, and Domestic Prices." *The Review of Economic Studies*, 86(6), 2356–2402.

Antràs, P., Chor, D., Fally, T., & Hillberry, R. (2012). "Measuring the Upstreamness of Production and Trade Flows." *American Economic Review*, 102(3), 412–416.

Autor, D. H., Dorn, D., & Hanson, G. H. (2013). "The China Syndrome: Local Labor Market Effects of Import Competition in the United States." *American Economic Review*, 103(6), 2121–2168.

Baqaee, D. R., & Farhi, E. (2019). "The Macroeconomic Impact of Microeconomic Shocks: Beyond Hulten's Theorem." *Econometrica*, 87(4), 1155–1203.

Baqaee, D. R., & Farhi, E. (2022). "Supply and Demand in Disaggregated Keynesian Economies with an Application to the COVID-19 Crisis." *American Economic Review*, 112(5), 1397–1436.

Barrot, J.-N., & Sauvagnat, J. (2016). "Input Specificity and the Propagation of Idiosyncratic Shocks in Production Networks." *The Quarterly Journal of Economics*, 131(3), 1543–1592.

Bhattacharyya, A., Kutlu, L., & Sickles, R. C. (2019). "Shadow Prices." In *The Palgrave Handbook of Economic Performance Analysis*, 511–540. Palgrave Macmillan, Cham.

Burstein, A., & Gopinath, G. (2014). "International Prices and Exchange Rates." In *Handbook of International Economics*, edited by G. Gopinath, E. Helpman, and K. Rogoff, Vol. 4, 391–451. Amsterdam: Elsevier.

Carvalho, V. M. (2014). "From Micro to Macro: The Case of Production Networks." *Journal of Economic Perspectives*, 28(4), 23–48.

Carvalho, V. M., Nirei, M., Saito, Y. U., & Tahbaz-Salehi, A. (2021). "Supply Chain Disruptions: Evidence from the Great East Japan Earthquake." *The Quarterly Journal of Economics*, 136(2), 1255–1321.

di Giovanni, J., Kalemli-Özcan, Ş., Silva, A., & Yildirim, M. A. (2022). "Global Supply Chain Disruptions and Inflation during the Pandemic." *NBER Working Paper* No. 30240.

Feenstra, R. C. (1994). "New Product Varieties and the Measurement of International Prices." *American Economic Review*, 84(1), 157–177.

Ferrari, A. (2025). "Inventories, Demand Shocks Propagation, and Amplification in Supply Chains." *Working Paper*.

Fontagné, L., Guimbard, H., & Orefice, G. (2022). "Tariff-based product-level trade elasticities." *Journal of International Economics*, 137, 103593.

Gabaix, X. (2011). "The Granular Origins of Aggregate Fluctuations." *Econometrica*, 79(3), 733–772.

Hummels, D., Jørgensen, R., Munch, J., & Xiang, C. (2014). "The Wage Effects of Offshoring: Evidence from Danish Matched Worker-Firm Data." *American Economic Review*, 104(6), 1597–1629.

Jones, C. I. (2011). "Intermediate Goods and Weak Links in the Theory of Economic Development." *American Economic Journal: Macroeconomics*, 3(2), 1–28.

Katz, L. (1953). "A new status index derived from sociometric analysis." *Psychometrika*, 18(1), 39–43.

Macchiavello, R. (2022). "Relational Contracts and Development." *Annual Review of Economics*, 14, 337–362.

Miller, R. E., & Blair, P. D. (2022). *Input-Output Analysis: Foundations and Extensions*. 3rn Edition. Cambridge University Press.

Nunn, N. (2007). "Relationship-specificity, incomplete contracts, and the pattern of trade." *The Quarterly Journal of Economics*, 122(2), 569–600.

Pasten, E., Schoenle, R., & Weber, M. (2020). "The Propagation of Monetary Policy Shocks in a Heterogeneous Production Economy." *Journal of Monetary Economics*, 116, 1–22.

Santacreu, A. M., & LaBelle, J. (2022). "Supply Chain Disruptions and Inflation during the COVID-19 Pandemic." *Federal Reserve Bank of St. Louis Review*, 104(3), 211–232.

Weitzman, M. L. (1974). "Prices vs. Quantities." *The Review of Economic Studies*, 41(4), 477–491.

A GVC Structure and Alternative Mechanisms

To further elucidate the role of network topology in modulating shock transmission, this section presents an extended analysis that incorporates a suite of alternative structural indicators. We examine whether the "structural buffer effect" and "network amplification" documented in the main text are truly driven by network centrality or whether they serve as proxies for other product-level and market-specific characteristics. To this end, we introduce three additional controls that reflect prominent dimensions of trade and production: upstreamness, market concentration, and market power.

The first indicator, upstreamness, measures the average distance of a product from final demand in terms of production stages. Following the recursive definition of Antràs et al. (2012), we define the upstreamness of country-sector i as:

$$U_i = 1 + \sum_j b_{ij} U_j \Rightarrow U = (I - B)^{-1}\mathbf{1} \tag{A.1}$$

where b_{ij} represents the share of country-sector i's output sold to country-sector j as an intermediate input. Second, to control for market structure and competition within specific destinations, we calculate the Herfindahl-Hirschman Index (HHI) for each product-destination-year cell as:

$$HHI_{jkt} = \sum_i (100 \times s_{ijkt})^2 \tag{A.2}$$

where $s_{ijkt} = v_{ijkt} / \sum_i v_{ijkt}$ is the market share of exporter i in destination j for product k at time t. Finally, we account for the overall global importance of an exporter-product pair using the global exporter share:

$$s_{ikt} = \frac{\sum_j v_{ijkt}}{\sum_i \sum_j v_{ijkt}} \tag{A.3}$$

where v_{ijkt} denotes the trade value for the corresponding flow. These structural indicators are lagged by one year and then integrated into our primary empirical specifications—defined in Equations (6) and (7) and their extensions incorporating COVID-19 interaction terms—to mitigate potential contemporaneous endogeneity and isolate the unique contribution of topological centrality. To ensure that our results are not driven by extreme observations common in high-resolution trade data, we trim all structural variables—centrality, upstreamness, HHI, and global exporter share—at the 0.1st and 99.9th percentiles.

Table A.1 reports the first-stage price pass-through results under these expanded specifications. The coefficient on the interaction between the negative supply shock and network centrality remains positive and highly significant at 0.0034 ($p < 0.01$), even when competing with these alternative indicators. Notably, the interaction with upstreamness is statistically insignificant across both directional subsamples. This null result provides critical evidence that the structural buffer effect we identify is not merely a proxy for a product's classification as a primary

commodity or raw material, but is specifically linked to its topological pervasiveness as a systemic common input.

Furthermore, we find that alternative structural variables exhibit distinct and asymmetric roles in price formation at the country-product level. For negative supply shocks, the interaction with HHI is negative and significant, whereas for positive shocks, it is positive and significant. This marked asymmetry suggests that higher market concentration within a destination market amplifies price surges during scarcity while simultaneously dampening price declines during gluts, a pattern consistent with standard theoretical predictions regarding the exercise of market power. Such behavior underscores the presence of downward price rigidity in intermediate goods markets and reflects the strategic pricing behaviors associated with market concentration.

In contrast, the global export share of a country-product pair exhibits a buffering role for negative shocks while facilitating greater pass-through for positive shocks. This behavior suggests that dominant country-product pairs may prioritize global market share stability or internalize cost fluctuations to preserve relational rents. The robust survival of the centrality coefficient amidst these competing channels confirms that the network's structural topology constitutes a fundamental and independent mechanism for price stabilization in global value chains.

The second-stage quantity adjustments, presented in Table A.2, reinforce the independence of the network amplification mechanism. For the negative shock subsample, the baseline Armington elasticity is estimated at -5.927. Crucially, the coefficient on the interaction between instrumented price changes and network centrality remains robust at -0.4033. This confirms that central goods trigger amplified quantity adjustments through downstream chains of substitution, even when controlling for alternative structural determinants. This persistent amplification cannot be explained by production distance or global market power, as evidenced by the concurrent inclusion of upstreamness and global export share.

While upstreamness remains insignificant, destination market concentration (HHI) exhibits a robust and symmetric dampening effect, with positive coefficients of 0.2342 for positive shocks and 0.2779 for negative shocks. This indicates that highly concentrated markets are structurally less responsive to price signals regardless of the shock's direction. Furthermore, global export share exhibits a statistically significant amplification effect that is notably stronger for negative shocks (-0.0011) compared to positive ones (-0.0003), although its economic significance is secondary to that of topological centrality.

Definitive evidence of the structural regime shift induced by the global supply chain crisis is documented in the triple interaction analysis in Table A.3. We define the post-pandemic recovery period as 2021–2022, purposefully excluding the idiosyncratic volatility of 2020 to isolate the persistent structural shifts in the production network. The results reveal that the crisis paralyzed not only the topological adjustment mechanisms but also the functional roles traditionally provided by market structure. In Stage 1, the price buffering effect afforded by global export share is effectively eliminated during the recovery period, as indicated by a triple

Table A.1. Price pass-through with alternative structural controls

Dep. variable:	Change in import price ($\Delta \ln p$)			
	Baseline	Asymmetry	Positive	Negative
	(1)	(2)	(3)	(4)
Supply shock (η)	−0.0070***	−0.0094***	−0.0139***	−0.0050**
	(0.0017)	(0.0017)	(0.0027)	(0.0020)
$\eta\times$ Pos. shock flag		0.0062***		
		(0.0012)		
$\eta\times$ Centrality			0.0009	0.0034***
			(0.0009)	(0.0006)
Additional Interactions with η:				
× Upstreamness			0.0003	−0.0006
			(0.0009)	(0.0008)
× HHI			0.0031***	−0.0025***
			(0.0006)	(0.0004)
× Exp. Market Share			−3.82e-6*	6.55e-6***
			(2.06e-6)	(6.01e-7)
Fixed effects:				
Importer × Year	Yes	Yes	Yes	Yes
Exporter × Year	Yes	Yes	Yes	Yes
Industry × Year	Yes	Yes	Yes	Yes
Observations	124,344,338	124,344,338	48,553,597	75,790,741
R-squared	0.00917	0.00917	0.00923	0.00945

Notes: The table reports estimated coefficients from first-stage price pass-through regressions. The sample and fixed-effects specifications are the same as those in Table 1 (1995–2023). Column (1) presents the baseline pass-through, and Column (2) examines the asymmetry between positive and negative shocks. Columns (3) and (4) include interactions of the supply shock with centrality, upstreamness, the HHI of exporter concentration in the destination market, and the exporter's market share. The HHI is calculated at the importer-product-year level and scaled by 1,000. The exporter's market share is expressed in percentage points. Standard errors in parentheses are clustered at the exporter and industry levels. ***, **, and * denote significance at the 1, 5, and 10 percent levels.

Table A.2. Demand elasticity with alternative structural controls

	IV-2SLS				OLS
Dep. variable: $\Delta \ln q$	Baseline (1)	Asymmetry (2)	Positive (3)	Negative (4)	Baseline (5)
Price change ($\Delta \ln \hat{p}$)	−4.731***	−5.535***	−2.639***	−5.927***	−0.6582***
	(0.7138)	(0.8101)	(0.6618)	(0.6689)	(0.0135)
$\Delta \ln \hat{p}\times$ Centrality			−0.0436	−0.4033*	
			(0.1038)	(0.2369)	
Add. Interactions with $\Delta \ln \hat{p}$*:*					
× Upstreamness			0.2648	0.2089	
			(0.1794)	(0.2132)	
× HHI			0.2342***	0.2779***	
			(0.0539)	(0.0614)	
× Exp. Market Share			−0.0003***	−0.0011*	
			(0.0001)	(0.0006)	
Fixed effects:					
Importer × Year	Yes	Yes	Yes	Yes	Yes
Exporter × Year	Yes	Yes	Yes	Yes	Yes
Industry × Year	Yes	Yes	Yes	Yes	Yes
Observations	124,344,338	124,344,338	48,553,597	75,790,741	124,344,338
1st-stage F (Price)	1,426.9	769.51	103.99	457.08	–

Notes: The table reports estimated coefficients from second-stage demand elasticity regressions. The sample and fixed-effects specifications are the same as those in Table 2 (1995–2023). Columns (1) to (4) instrument import price changes and their interactions with supply shocks (η) and corresponding interactions. Column (5) provides OLS estimates for comparison. Columns (3) and (4) include interactions of the instrumented price change with centrality, upstreamness, the HHI of exporter concentration in the destination market, and the exporter's market share. The HHI is calculated at the importer-product-year level and scaled by 1,000, and the exporter's market share is expressed in percentage points. Standard errors in parentheses are clustered at the exporter and industry levels. ***, **, and * denote significance at the 1, 5, and 10 percent levels.

interaction term (−7.27e-6) that almost perfectly offsets the baseline coefficient. In Stage 2, a similar pattern of systemic paralysis emerges for quantity adjustments. The pre-pandemic centrality amplification effect of −0.4185 is neutralized by a positive triple interaction term of 0.4383, with a Wald test of the hypothesis that the sum of these coefficients equals zero yielding a p-value of 0.8978. Correspondingly, the quantity-side effects for both destination market concentration (HHI) and global export share exhibit significant offsets during the recovery period, suggesting that the conventional market-based determinants of trade adjustments were rendered ineffective by the severity of the supply disruptions.

Collectively, these findings provide rigorous statistical proof that pervasive physical bottlenecks choked off the structural pathways typically afforded by network centrality and market prominence. This systemic paralysis confirms the latent risk of signal attenuation, where the erosion of market-based stabilizers masks the accumulation of severe physical shortages, creating a hidden vulnerability in the global production network.

Table A.3. GVC Dynamics during the COVID-19 Recovery: Extended Specifications

Dep. variable:	Stage 1: Price $\Delta \ln p$ (1)	Stage 2: Quantity $\Delta \ln q$ (2)
Supply shock (η)	−0.0054**	
	(0.0021)	
Price change ($\Delta \ln \hat{p}$)		−5.705***
		(0.6262)
Main Mechanism: Network Centrality		
Shock/Price × Centrality	0.0033***	−0.4185
	(0.0007)	(0.2587)
Shock/Price × Centrality × COVID	−0.0009	0.4383
	(0.0029)	(0.3034)
Structural Controls:		
Shock/Price × Upstreamness	−0.0003	0.1944
	(0.0009)	(0.2548)
Shock/Price × Upstreamness × COVID	−0.0026	0.1285
	(0.0024)	(0.2621)
Shock/Price × HHI	−0.0025***	0.2874***
	(0.0004)	(0.0672)
Shock/Price × HHI × COVID	0.0005	−0.1570**
	(0.0008)	(0.0659)
Shock/Price × Exp. Market Share	6.98e-6***	−0.0013
	(6.44e-7)	(0.0009)
Shock/Price × Exp. Market Share × COVID	−7.27e-6***	0.0014*
	(1.93e-6)	(0.0008)
Fixed Effects	Imp-Year, Exp-Year, Ind-Year	
Observations	71,681,682	71,681,682
1st-stage F-statistics :		
$\Delta \ln \hat{p}$	–	249.73
$\Delta \ln \hat{p}$× Centrality	–	1,314.6
$\Delta \ln \hat{p}$× Centrality × Post	–	8,442.4
$\Delta \ln \hat{p}$× Upstreamness	–	980.13
$\Delta \ln \hat{p}$× Upstreamness × Post	–	3,549.3
$\Delta \ln \hat{p}$× HHI	–	3,202.8
$\Delta \ln \hat{p}$× HHI × Post	–	5,487.5
$\Delta \ln \hat{p}$× Exp. Market Share	–	2,775.3
$\Delta \ln \hat{p}$× Exp. Market Share × Post	–	25,833.1

Notes: The table reports results from a triple interaction specification to examine structural shifts during the COVID-19 recovery period. The sample covers 1995–2023, and "COVID" is a dummy variable equal to one for the years 2021–2022. Column (1) presents the first-stage price pass-through, and Column (2) presents the second-stage quantity adjustments. All specifications are restricted to negative supply shocks ($\eta < 0$) and include interactions with centrality, upstreamness, the HHI of exporter concentration in the destination market, and the exporter's market share. The HHI is calculated at the importer-product-year level and scaled by 1,000, and the market share is expressed in percentage points. Standard errors in parentheses are clustered at the exporter and industry levels. ***, **, and * denote significance at the 1, 5, and 10 percent levels.